Chemical Engineering Journal 486 (2024) 150281

Contents lists available at ScienceDirect

Chemical Engineering Journal

journal homepage: www.elsevier.com/locate/cej

Electrodialysis for efficient antisolvent recovery in precipitation of critical metals and lithium-ion battery recycling

Simon B.B. Solberg [a], Lucía Gómez-Coma [d], Øivind Wilhelmsen [b], Kerstin Forsberg [c], Odne S. Burheim [a,*]

[a] Norwegian University of Science and Technology, Department of Energy and Process Engineering, Høgskoleringen 1, Trondheim, NO-7491, Norway
[b] Department of Chemistry, Norwegian University of Science and Technology, Høgskoleringen 1, Trondheim, NO-7491, Norway
[c] KTH Royal Institute of Technology, Department of Chemical Engineering, Teknikringen 42, Stockholm, 114 28, Sweden
[d] University of Cantabria, Department of Chemical and Biomolecular Engineering, Av. Los Castros 46, Santander, 39005, Spain

ARTICLE INFO

Keywords:
Electrodialysis
Non-equilibrium thermodynamics
Ion-exchange membranes
Ethanol recycling
Demineralisation
Transference numbers

ABSTRACT

It has proven effective to recover metal compounds from aqueous mixtures by use of antisolvents; organic compounds that induce selective precipitation. A challenge with antisolvents is that they are both costly to produce and recover on an industrial scale. In recycling of lithium-ion batteries and recovering critical metals, we find that electrodialysis can be a competitive method for purifying and recycling antisolvents. In this study we investigate the use of electrodialysis to separate salt and water from a ternary solution of water, KCl and ethanol. A coupled non-equilibrium electrochemical model is developed to understand how such systems may be operated, designed, and which characteristics that are required for the ion exchange membranes. We demonstrate how the water transference coefficients of the membranes should be tuned in the process optimisation and why membrane property design is crucial to the success of this concept. Residual mixtures from antisolvent precipitation, with ethanol (EtOH) solvent weight fractions around 0.6-0.7, can be demineralised and the EtOH fraction increased by 0.1-0.2 at an energy requirement of 60-200 kWh m^{-3}_{EtOH} by use of electrodialysis. In an example application of the concept, aqueous KCl is precipitated by recycled ethanol in a cyclic process, requiring 0.161 kWh mol^{-1}_{KCl}. This example case considers complete ethanol rejection by the membranes and abundant water co-transport, characterised by the transference coefficients: $t_w = 15$ and $t_a = 0$ for water and EtOH respectively. The findings pave the way for new applications with aqueous mixtures of critical metals.

1. Introduction

Energy storage systems are a prerequisite in mitigating the intermittency of renewable resources [1,2]. Such systems store excess energy produced during high generation periods and release it when renewable sources are unable to meet the demand. Various storage technologies, such as pumped hydro storage [3], compressed air energy storage [4,5], and battery technologies [6–8] are being developed and implemented to facilitate efficient energy management and ensure a consistent power supply. First and foremost, the rapid market growth of portable electronic devices, electric vehicles, and renewable energy systems has fuelled the need for efficient and reliable energy storage solutions. Lithium-ion batteries have emerged as a preferred choice due to their high energy density, long cycle life, and lightweight nature, making them well-suited for a wide range of applications. The demand for lithium-ion batteries and similar battery technologies is therefore expected to increase drastically in the near future [9–11].

The widespread adoption of modern battery technology has also raised concerns regarding the necessity for effective recycling practices. Recycling of lithium-ion batteries is currently considered to be in an early stage and far from reaching maturity [12]. This challenge is becoming increasingly important due to the rising supply chain constraints for critical materials and a shift in policies towards increased material circularity, driven by environmental concerns [13]. Therefore, recycling has become an essential and urgently needed part of the value chain to achieve sustainable development [14,15].

Antisolvent precipitation, also known as solvent displacement crystallisation, is a target specific hydrometallurgical alternative that offers interesting possibilities for controlling the crystallisation process. This technique is based on altering the solubility of the solute and creating a supersaturated solution by introducing a water-miscible organic solvent to induce precipitation of the solute [16]. While it is used

* Corresponding author.
E-mail address: burheim@ntnu.no (O.S. Burheim).

https://doi.org/10.1016/j.cej.2024.150281
Received 7 January 2024; Received in revised form 4 March 2024; Accepted 8 March 2024
Available online 11 March 2024

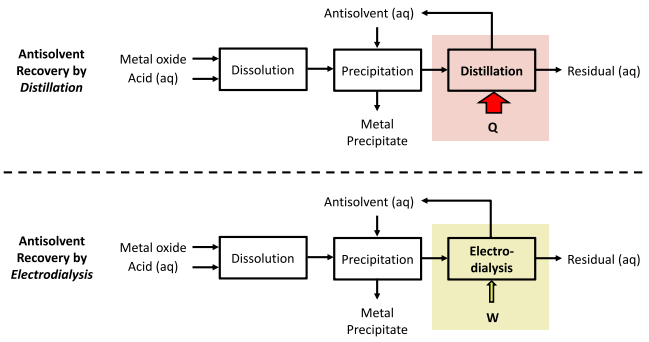

Fig. 1. Illustration of two options for antisolvent recovery and associated utilities. Recovery by distillation requires a heat duty, Q, while the electrodialysis process requires electrical work, W.

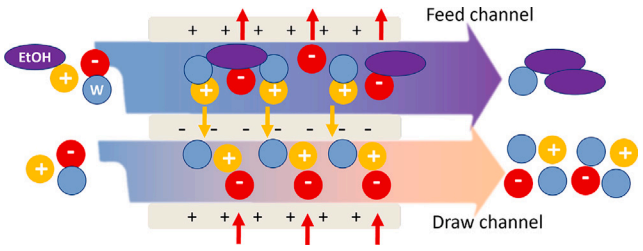

Fig. 2. A sketch of a concept that uses electrodialysis for antisolvent recovery. The sketch illustrates a section of an electrodialysis cell, where a mixture of antisolvent, water and salt enters in the feed channel and salt and water enters in the draw channel. The two feed channels are separated by cation-exchange membrane and anion-exchange membranes.

Table 1
The absolute water transference coefficients, $|t_w|$, for various commercial cation-exchange membranes (CEMs) and anion-exchange membranes (AEMs) in cells with binary mixtures of water and salt.

Membrane	Type	Ion (Salt)	$\|t_w\|$	
Nafion 117	CEM	H^+ (HCl)	9	[38]
Nafion 117	CEM	Li^+ (LiCl)	16	[38]
Nafion 117	CEM	Na^+ (NaCl)	3	[38]
Nafion 117	CEM	K^+ (KCl)	5	[38]
Selemion CMVN	CEM	K^+ (KCl)	4	[39]
Nafion 117	CEM	Mg^{2+} ($MgCl_2$)	14	[40]
Fumasep FAD	AEM	Cl^- (NaCl)	6	[41]
Selemion AMVN	AEM	Cl^- (KCl)	4	[39]

extensively in the pharmaceutical industry, it could also be a promising option for battery recycling [16,17]. Aktas et al. proposed a route for the hydrometallurgical recycling of lithium-ion batteries using ethanol (EtOH) [18]. In this case, it is essential to recover the antisolvent after solute precipitation to reduce chemical waste. After reclaiming the precipitated solute, an available approach for further processing of the ternary mixture (consisting of water, antisolvent and small amounts of remaining salt) is distillation of the antisolvent. However, the energy requirements for the evaporative separation of H_2O-EtOH mixtures are relatively high. Distillation processes using feed mixtures containing 5–10%v/v EtOH, with and without added extractive salt, have energy requirements in the range 1000–4200 kWh m^{-3} of produced anhydrous ethanol [19]. However, the enthalpy of evaporation of pure EtOH is approximately 190 kWh m^{-3} [20]. Membrane processes such as reverse osmosis are largely preferred compared to evaporative processes for desalination and the production of potable water, due to low capital costs and energy consumption [21]. Similarly, a promising alternative to distillation of EtOH is the separation of salt and water from EtOH by the electro-membrane process of electrodialysis.

Electrodialysis finds wide application in separation processes containing ionic species, such as industrial waste-water treatment and desalination/demineralisation [22–27]. Demineralisation with electrodialysis has been applied in a wide range of food systems containing dissolved salts and other organic solutes [28–36]. Electrodialysis is apt for the separation of ions of differing valencies and can therefore be useful for metal recovery, but ions featuring the same charge valency are difficult to separate [37]. The energy efficiency of the electrodialysis process also heavily depends on the abundance of ionic species in the feed mixture [27]. In these applications, it is typically necessary to selectively remove charged species while retaining organic solutes or solvents.

The concept investigated in this work requires a substantial co-transport of water, in order to refine the EtOH in the demineralised feed mixture. Electrochemical cells for electrodialysis use an alternating configuration of cation- and anion-exchange membranes, with applied electric current in the direction perpendicular to the membranes. Electrolyte solutions flow parallel to the membranes, such that every other solution compartment is depleted of salt as the mixture flows from inlet to outlet. General process flow charts for the antisolvent recycling by distillation and by electrodialysis are shown in Fig. 1. The hydrometallurgical recycling process for lithium-ion batteries proposed by Aktas et al. is one intended application of such a demineralisation process using electrodialysis. Aqueous mixtures of critical metals and antisolvents such as Li_2SO_4, $CoSO_4$ and EtOH are then of primary interest. However, thermodynamic data for aqueous mixtures of critical metals, antisolvents and sulphuric acid in the literature are scarce. We will therefore investigate a model mixture of potassium chloride (KCl), water and ethanol, due to the availability of thermodynamic data for the ternary mixture. Using a stream of KCl, H_2O and EtOH, we aim to force KCl and H_2O through the ion-exchange membranes, leaving a purified EtOH stream behind. The concept is illustrated in Fig. 2.

Studies have shown that ionic species carry significant shells of water molecules while migrating through commercial ion-exchange membranes (IEMs), as quantified by the water transference coefficient [38,39,41–43]. This phenomenon is often referred to as electroosmosis. Values for various binary mixtures of salt and water in cells with commercial membranes are shown in Table 1. It is evident that the magnitude of the electroosmotic transport of water is both membrane and ion specific. The proposed electrodialysis process is similar in nature to osmotically assisted reverse osmosis, which has been applied to the separation of, for example, water and EtOH [44]. Selective membranes have been produced by several researchers for the removal of water from a feed mixture containing organic compounds [44–49]. In particular, they find a water and antisolvent flux dependent on membrane characteristics, antisolvent choice and concentration. However, the reverse osmosis process is unable to demineralise the feed mixture to the same extent as is possible with electrodialysis. For that reason, we will treat the transference coefficients as variables, in order to identify the properties of the ion-exchange membrane that can realise the electrodialysis concept. If ions preferentially bind and co-migrate with water over antisolvent, an aqueous membrane process such as electrodialysis may prove useful for the purification of antisolvent.

This work aims to describe and investigate the use of electrodialysis for antisolvent recovery through a theoretical framework based on non-equilibrium thermodynamics, accounting for the coupling of fluxes. This framework is used to simulate the simplified mixture flow through an electrodialysis unit cell consisting of two electrolyte compartments, one cation- and one anion-exchange membrane. Particularly, we treat the transference coefficients of water and EtOH as variables, i.e. the coupling between current density and solvent fluxes, and in this way investigate the process efficacy with different membrane properties. Fick diffusion coefficients and electric resistances are estimated from experiments to supplement the numerical model. The model will be used to evaluate the feasibility of the concept, and in particular estimate the energy consumption for EtOH purification.

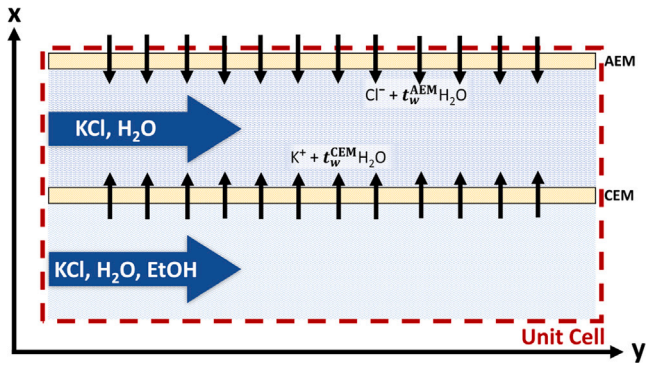

Fig. 3. Illustration of a unit cell consisting of one cation-exchange membrane, one anion-exchange membrane, one feed channel containing KCl, EtOH and H_2O, and one draw channel containing KCl and H_2O.

2. Thermodynamic framework

2.1. Transport relations in a three component electrodialysis system

We consider the transport phenomena in the smallest repeating section of an electrodialysis cell, known as a unit cell. Such a section is illustrated in Fig. 3. We consider area averaged component profiles in the y-direction, parallel to the membranes, using a laboratory frame of reference. Frictional losses are not taken into account, and temperature variations are neglected.

The steady state fluxes of components and charge in the three component electrolyte mixture are described by non-equilibrium thermodynamics [50,51]. Isothermal, isobaric and electroneutral conditions are assumed for the whole electrochemical system, and all irreversible phenomena in the y-direction, i.e. the direction of convection, are neglected. In the x-direction (perpendicular to the membranes), the four coupled fluxes are described by the following flux-force relationship:

$$\begin{bmatrix} J_s \\ J_w \\ J_a \\ j \end{bmatrix} = -\frac{1}{T}\begin{bmatrix} L_{ss} & L_{sw} & L_{sa} & L_{s\phi} \\ L_{ws} & L_{ww} & L_{wa} & L_{w\phi} \\ L_{as} & L_{aw} & L_{aa} & L_{a\phi} \\ L_{a\phi} & L_{\phi w} & L_{\phi a} & L_{\phi\phi} \end{bmatrix}\begin{bmatrix} \mathrm{d}\mu_s/\mathrm{d}x \\ \mathrm{d}\mu_w/\mathrm{d}x \\ \mathrm{d}\mu_a/\mathrm{d}x \\ \mathrm{d}\phi/\mathrm{d}x \end{bmatrix} \tag{1}$$

where J_k and $\mathrm{d}\mu_k/\mathrm{d}x$ are the molar flux of component k and the spatial derivative of the chemical potential across the membrane interface, j is the current density, T is the absolute temperature, ϕ is the measurable electric potential, and the subscripts s, w and a denote salt, water and antisolvent (in this case EtOH) respectively. The L_{ij} matrix contains phenomenological coefficients, in which the off-diagonal elements give the magnitude of the coupling between fluxes, and the diagonal elements are related to the main transport effects such as diffusion and conductivity [50,51]. In this treatment, phenomenological coefficients are assumed to be constant for the entire membrane interior.

We neglect concentration polarisation in the x-direction of the channels in order to simplify the system. This effect is known to significantly influence the current density that can be applied at a certain flow velocity [23], however we focus here on the separation capability of the membranes themselves. The current density from Eq. (1) may be re-arranged with respect to the electric potential difference, yielding:

$$\frac{\mathrm{d}\phi}{\mathrm{d}x} = -\frac{L_{\phi s}}{L_{\phi\phi}}\frac{\mathrm{d}\mu_s}{\mathrm{d}x} - \frac{L_{\phi w}}{L_{\phi\phi}}\frac{\mathrm{d}\mu_w}{\mathrm{d}x} - \frac{L_{\phi a}}{L_{\phi\phi}}\frac{\mathrm{d}\mu_a}{\mathrm{d}x} - \frac{T}{L_{\phi\phi}}j \tag{2}$$

The ratios of phenomenological coefficients can be identified as the transference coefficients, t_k, and resistivity, r_Ω, through:

$$t_k = F\left(\frac{J_k}{j}\right)_{\mathrm{d}\mu/\mathrm{d}x=0} = F\frac{L_{\phi k}}{L_{\phi\phi}} \tag{3}$$

$$r_\Omega = -\left(\frac{\mathrm{d}\phi/\mathrm{d}x}{j}\right)_{\mathrm{d}\mu/\mathrm{d}x=0} = \frac{T}{L_{\phi\phi}} \tag{4}$$

where the Onsager reciprocal relation was used in Eq. (3), and the subscript $\mathrm{d}\mu/\mathrm{d}x = 0$ means uniform composition for all components. The membrane and ternary mixture resistance are calculated using empirical relations shown in Appendix B. The transference coefficients describe the number of moles of a component transported per mole of electrons passing through the external circuit [50,51]. In the proposed antisolvent recovery process using electrodialysis, it is necessary to use membranes with high water and low antisolvent transference coefficients, so that salt and water is transferred from the feed to the draw solution leading to an increasing fraction of antisolvent in the feed. The relation between the salt transference coefficient and the fractions of the current carried by each ionic species depends on the choice of electrodes that measure the electric potential [50]. In this treatment, we do not make this relation explicit and instead use the salt transference coefficient. Nevertheless, for a unit cell consisting of one CEM and AEM, the sum of the membranes' salt transference coefficients in a single salt electrolyte mixture cannot exceed unity. Physically, this means that the passage of one mole of electrons in the external circuit can lead to a maximum of one mole of salt (perfectly selective membranes) migrating from the feed to the draw solution.

Assuming that the chemical potential gradients in all membranes are linear, Gibbs-Duhem's equation takes the form:

$$c_s\frac{\mathrm{d}\mu_s}{\mathrm{d}x} + c_w\frac{\mathrm{d}\mu_w}{\mathrm{d}x} + c_a\frac{\mathrm{d}\mu_a}{\mathrm{d}x} = 0 \tag{5}$$

where c_k is the molar concentration of component k. This relation is used to eliminate the chemical potential difference of EtOH. The measurable electric potential difference across one membrane becomes:

$$-F\frac{\mathrm{d}\phi}{\mathrm{d}x} = \left(t_s - \frac{c_s}{c_a}t_a\right)\frac{\mathrm{d}\mu_s}{\mathrm{d}x} + \left(t_w - \frac{c_w}{c_a}t_a\right)\frac{\mathrm{d}\mu_w}{\mathrm{d}x} + Fr_\Omega j \tag{6}$$

Eq. (6) reduces to the ohmic contribution for the bulk electrolyte mixture in each channel, where concentration polarisation is neglected. When integrated across the membranes, the electric potential difference for one unit cell at any y-position becomes:

$$\begin{aligned} -F\Delta\phi_{\mathrm{unit}} =& Fj(R_{\mathrm{CEM}} + R_{\mathrm{AEM}} + R_{\mathrm{feed}} + R_{\mathrm{draw}}) \\ &+ (t_1^{\mathrm{CEM}} - t_1^{\mathrm{AEM}})\Delta\mu_s + (t_2^{\mathrm{CEM}} - t_2^{\mathrm{AEM}})\Delta\mu_w \end{aligned} \tag{7}$$

where Δ refers to the difference across the membranes, the area resistance is $R = \delta_m r_\Omega$ where δ_m is the membrane thickness and subscripts CEM, AEM, feed, draw refer to the cation exchange membrane, anion exchange membrane, bulk feed and bulk draw solutions respectively. Moreover,

$$t_1 \approx \overline{\left(t_s - \frac{c_s}{c_a}t_a\right)} \quad \text{and} \quad t_2 \approx \overline{\left(t_w - \frac{c_w}{c_a}t_a\right)} \tag{8}$$

where $\overline{()}$ refers to the average taken across the membrane. We are now left with an equation that allows determining the electric work of separating the salt and water from the antisolvent as a function of the chemical potential differences across the membranes. These chemical potential differences can be calculated if the thermodynamic activities are known. Ternary mixture activities of KCl, H_2O and EtOH were measured by Yang et al., Dill et al., Mussini et al. and Lopes et al. [52–55] by the use of concentration cells, formation cells and vapour pressure measurements. The activity at any relevant composition is here found by interpolation.

We now turn to the component fluxes of Eq. (1). Eq. (2) is substituted into the component flux equations, yielding:

$$J_k = -\frac{1}{T}\left[l_{ks}\frac{\mathrm{d}\mu_s}{\mathrm{d}x} + l_{kw}\frac{\mathrm{d}\mu_w}{\mathrm{d}x} + l_{ka}\frac{\mathrm{d}\mu_a}{\mathrm{d}x} - T\frac{t_k}{F}j\right] \tag{9}$$

where the new phenomenological coefficients are related to the initial coefficients through: $l_{ij} = L_{ij} - L_{i\phi}L_{\phi j}/L_{\phi\phi}$. Diffusive transport carrying no net charge is suspected to play a minor role compared to component transport by migration in the case of a once-through demineralisation.

After introducing the Gibbs-Duhem equation in Eq. (9), the Fick diffusion coefficients are identified in relation to the phenomenological coefficients by using:

$$D_{ks} = -\left(\frac{J_k}{\mathrm{d}c_s/\mathrm{d}x}\right)_{j=0,\mathrm{d}c_w/\mathrm{d}x=0}$$
$$D_{kw} = -\left(\frac{J_k}{\mathrm{d}c_w/\mathrm{d}x}\right)_{j=0,\mathrm{d}c_s/\mathrm{d}x=0} \quad (10)$$

where D_{ks} is the Fick diffusion coefficient of component k for diffusion driven by a concentration difference of salt, and D_{kw} is the coefficient for diffusion driven by a water concentration difference. The Fick diffusion coefficients are not symmetric, $D_{ws} \neq D_{sw}$ [56]. For one membrane, the component fluxes finally become:

$$J_k = -D_{ks}\frac{\mathrm{d}c_s}{\mathrm{d}x} - D_{kw}\frac{\mathrm{d}c_w}{\mathrm{d}x} + t_k\frac{j}{F} \quad (11)$$

Assuming steady-state and integrating across the membrane, we o btain:

$$J_k \approx -D_{ks}\frac{\Delta c_s}{\delta_m} - D_{kw}\frac{\Delta c_w}{\delta_m} + \overline{t_k}\frac{j}{F} \quad (12)$$

To ease notation, we shall omit the bar from $\overline{t_k}$ in the following treatment.

2.2. Mole balances and energy expenditure of antisolvent recovery

The area averaged molar flow of each component along the y-direction of the feed channel (parallel to the membranes) is here described by steady state mole balances on the form:

$$\frac{\mathrm{d}N_k}{\mathrm{d}y} = \frac{A_m}{L}\left(J_k^{\mathrm{CEM}} - J_k^{\mathrm{AEM}}\right) \quad (13)$$

where N_k is the molar flow of component k and L is the length of the channel. Steady state is assumed for all subsystems of the cell. Introducing the flux relations yields:

$$\frac{\mathrm{d}N_k}{\mathrm{d}y} = \frac{2A_m}{L}\left(D_{ks}\frac{\Delta c_s}{\delta_m} + D_{kw}\frac{\Delta c_w}{\delta_m} - t_k\frac{j}{F}\right) \approx -2t_k\frac{A_m}{L}\frac{j}{F} \quad (14)$$

where the ion-exchange membranes are taken to have equal transference and Fick diffusion coefficients, and the last equality is a useful simplification if the diffusive transport is negligible. In such a case, an analytical solution of the differential equation is:

$$N_k(y) = N_k^0 - 2t_k\frac{A_m}{L}\frac{j}{F}y \quad (15)$$

where N_k^0 is the molar flow rate of component k at the inlet of the feed channel. In the case of electrodialysis with a single-pass flow configuration, the transport of components by migration is expected to be significantly higher than diffusive transport.

For an electrochemical cell in which the current density is controlled to ensure complete demineralisation of the feed solution, the introduction of a dimensionless coefficient is useful to describe the depletion of a component in the feed channel:

$$\zeta_k = 2t_k\frac{A_m}{N_k^0}\frac{j}{F} \quad (16)$$

This coefficient varies from zero to unity, corresponding to zero and complete depletion of the component in the feed channel, respectively. The applied current density is for all investigated cases determined based on next to complete depletion of the salt by the outlet of the cell, i.e. $\zeta_s = 0.99$. We refrain from using complete demineralisation in order for the resistance and salt chemical potential to remain finite.

The mixture composition may also be described in terms of molality, m_s (salt per kilogram of mixed solvent), and solvent weight fractions, $\omega_w + \omega_a = 1$. These are related to the molar flow rates by:

$$1 - \omega_a = \omega_w = \frac{N_w M_w}{N_w M_w + N_a M_a}$$
$$m_s = \frac{N_s}{N_w M_w + N_a M_a} \quad (17)$$

The electric power, P, applied to each unit cell is calculated by:

$$P = -\int_0^L \Delta\phi_{unit} j \, \mathrm{d}y \quad (18)$$

In order to compare the energy expenditure for electrodialysis with commercial distillation technology, we need also account for the electrode reactions. The ferricyanide-ferrocyanide electrode system is an example of a fairly reversible red-ox system, given its smooth reaction kinetics [57,58]. Therefore, the contribution from the electrode compartments to the power density is negligible.

Table 2
The electrochemical cell length (inlet to outlet), L, electrode/membrane area, A_m, channel width, w_{channel}, mass flow rate of solvent, F_{solv}, and the diffusion, D_k, and transference coefficients, t_k, of component k.

Parameter	Value	
D_{ss}	1×10^{-8} cm^2 s^{-1}	[59]
D_{sw}	1×10^{-9} cm^2 s^{-1}	[56,59]
D_{ww}	2×10^{-7} cm^2 s^{-1}	
D_{ws}	2×10^{-8} cm^2 s^{-1}	[56]
D_{as}	0 cm^2 s^{-1}	
D_{aw}	0 cm^2 s^{-1}	
t_s	0.5	
δ_m	100 μm	[60]
L	10 cm	[61]
A_m	100 cm^2	[61]
w_{channel}	270 μm	[61]
F_{solv}	0.27 g s^{-1}	[61]

3. Computational procedure

Essential parameters for the electrochemical system such as the cell geometry and mass flow rate of solvent are presented in Table 2. Here, the Fick diffusion coefficients are taken as constants. The main Fick diffusion coefficient of the salt represents a typical value based on measurements by Veerman et al. [59]. Two Fick diffusion coefficients of water and EtOH, D_{ww} and D_{aw}, in the Selemion CMVN and AMVN membranes are based on experimental investigation shown in Appendix A. Based on the poor diffusive coupling between water and EtOH we also assume poor EtOH coupling with the salt, $D_{as} = 0$. The remaining diffusion coefficients, D_{ws} and D_{sw}, are taken to be ten times smaller than the main coefficients, D_{ww} and D_{ss} respectively, based on the magnitude of Fick diffusion coefficients reported by Liu et al. for a chloroform-acetone-methanol mixture. Using these values, the magnitude of the diffusion transport is for any point along the length of the channel around 10^{-4}, whereas the transport by migration is on the order of magnitude of 10^{-3} to 10^{-1}. Therefore, diffusion is neglected and we investigate a unit cell described by the analytical solution presented in Eq. (15).

The molar flow rate of a component in the feed channel of one unit cell is therefore calculated by Eq. (15), and the flow rates in the draw channel may be calculated by taking the total flow rate of one component in the whole unit cell to be constant. The chosen solvent mass flow rate corresponds to a solvent velocity of approximately 1 cm s^{-1}. A co-current flow configuration is used, and the resulting molar flow rates parallel to the membranes are presented in terms of the new variables given in Eq. (17). The current density is chosen using Eq. (16), such that the amount of salt in the feed channel is reduced by 99% by the outlet of the cell, i.e. $\zeta_s = 0.99$. The membrane resistance used for energy calculations is derived from empirical relations based on experimental data shown in Appendix B.

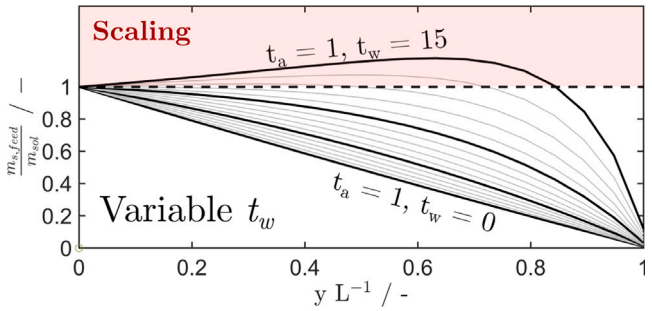

Fig. 4. The salt molality profile of the feed channel divided by the composition-dependent solubility limit, $m_{s,feed}/m_{sol}$. All curves are generated with $t_a = 1$, thick black lines show molality profiles generated with t_w increments of 5, and thin grey lines show intermediate cases. A red shaded area above $m_{s,feed}/m_{sol} = 1$ indicates cases in which scaling occurs.

All investigated cases are based on a feed mixture consisting of the remaining ternary mixture after precipitation of salt by EtOH addition. This mixture is then saturated with KCl at the electrodialysis cell inlet. The draw mixture always consists of 0.1 mol kg^{-1} KCl in pure water, with the same solvent mass flow rate as the feed. The water and EtOH transference coefficients of each individual membrane, t_w and t_a, and the initial solvent weight fraction of EtOH, $\omega_{a,in}$, serve as the main variables that are varied in this investigation. Varying the feed inlet solvent weight fraction of EtOH also varies the flow rate of salt through the empirical solubility relations shown in Appendix C, since the mixture is saturated. The initial feed composition in terms of molar flow rates in these various cases is:

$$\begin{aligned} N_s^0 &= m_{sol} F_{\text{solv}} \\ N_w^0 &= \frac{\omega_{w,in}}{M_w} F_{\text{solv}} \\ N_a^0 &= \frac{\omega_{a,in}}{M_a} F_{\text{solv}} \end{aligned} \tag{19}$$

where m_{sol} is the salt solubility in terms of molality, which is a function of EtOH solvent weight fraction, ω_a.

4. Results and discussion

4.1. Electrodialysis with a saturated feed solution

The investigated electrodialysis concept mainly builds on and further conceptualises a hydrometallurgical route for recycling spent Li-ion batteries. Studies by, for example, Aktas et al. investigate the recovery of critical metals from aqueous mixtures of acid leached battery components by precipitation using EtOH as an antisolvent [18]. Around 92% of the cobalt and 90% of the lithium were recovered as $CoSO_4$ and Li_2SO_4 by the addition of EtOH to a solvent weight fraction of approximately $\omega_a = 0.7$. The remaining mixture then contains water corresponding to $\omega_w = 0.3$, and is saturated with salt(s) of critical metal(s) at some non-neutral pH. We investigate the possibility of using electrodialysis to further process a similar, but simplified, mixture of saturated KCl in a mixed solvent of water and EtOH. The KCl electrolyte serves as an example salt in these calculations, due to the availability of thermodynamic data for this ternary mixture. The purpose of this is to demonstrate the feasibility of energy-efficient purification of EtOH with electrodialysis, so that the antisolvent may be reused for subsequent hydrometallurgical recycling.

Using a feed solution that is saturated with salt at the inlet of the electrodialysis cell, the water transference coefficient is limited in the sense that too much co-transport of water will increase the salt molality in the feed channel and induce precipitation on the membranes, i.e. scaling. Resulting profiles of the salt molality are shown for various membrane t_w values in Fig. 4. In this particular example,

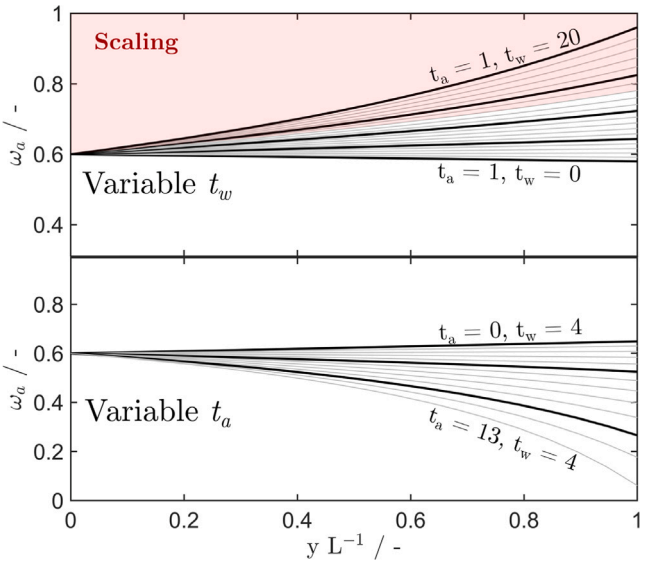

Fig. 5. The EtOH solvent weight fraction profiles, ω_a, from the inlet (y $L^{-1} = 0$) to the outlet (y $L^{-1} = 1$) of the feed channel, with variable t_w (top figure) and variable t_a (bottom figure). Thick black lines show profiles generated with transference coefficient increments of 5, while thin grey lines show intermediate cases. A red shaded area above $t_w = 11$ in the top figure indicates cases in which scaling occurs.

using an initial solvent weight fraction of EtOH of 0.6, an individual membrane water transference coefficient of above 11 will result in scaling inside the cell. At this EtOH weight fraction, the KCl solubility is $m_{sol} = 0.53$ mol kg^{-1}, cf. Appendix C.

The effect of varying the solvent transference coefficients is illustrated for the EtOH fraction in Fig. 5. In the case where each membrane in the cell has $t_w = 11$ and $t_a = 1$, the EtOH solvent weight fraction can be increased from $\omega_a = 0.6$ to 0.78 by demineralising the feed. In a hypothetical case where the ion-exchange membranes have higher water transference coefficients but also low EtOH transference, it may be necessary to add water to the feed solution in order to prevent scaling issues. Nevertheless, the EtOH transference coefficient has a large impact on the resulting feed composition. Due to the differing molar weights of water and EtOH, a EtOH transference coefficient of two leads to a mass flux comparable to that of H_2O with a water transference coefficient of four. This is further illustrated by two different cases. For a case of membranes with transference coefficients $t_w = 11$ and $t_a = 1$, the EtOH solvent weight fraction is increased by roughly: $\omega_{a,out} - \omega_{a,in} = 0.18$. In a case where the transference coefficients are $t_w = 4$ and $t_a = 13$, the EtOH fraction change is instead $\omega_{a,out} - \omega_{a,in} = -0.56$. Excellent rejection of the antisolvent is a necessary property of ion-exchange membranes for this electrodialysis concept to work.

The transference coefficient of EtOH is assumed low due to EtOH's poor ability to solvate KCl. Moreover, a small co-migration of phenol (10x smaller than the water flux) was found during the demineralisation by electrodialysis of aqueous mixtures of phenol and NaCl [26]. The co-transport of glycerol during electrodialysis of a $NaNO_3$ mixture was measured by Zelman et al., who found a glycerol transference coefficient of around 0.1. Still, there is reason to assume that the solvent transference coefficients vary with EtOH content, with $t_a = 0$ when $w_a = 0$ and $t_w = 0$ when $w_a = 1$. In the reverse osmosis system for dehydration and purification of EtOH investigated by Chiao et al., the membrane's ability to reject EtOH decreased with increasing EtOH content in the feed. The antisolvent rejection also varied with membrane characteristics and antisolvent type [44]. Exact transport relations must be determined for any salt and composition for which the demineralisation process is of interest.

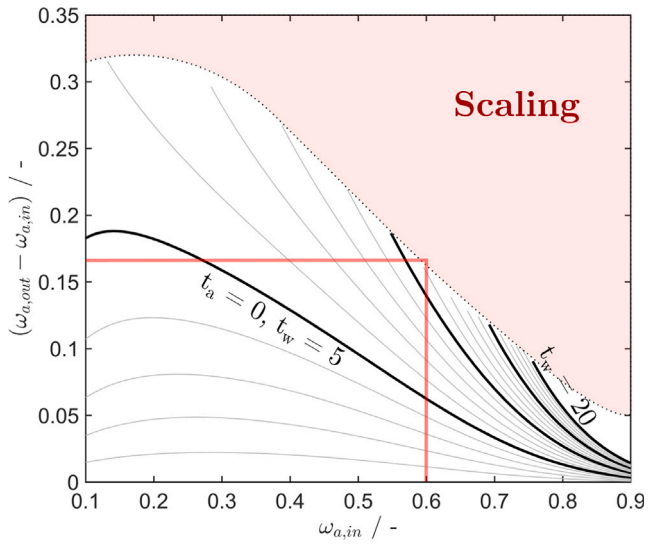

Fig. 6. The change in EtOH solvent weight fraction over the course of the process, $(\omega_{a,out} - \omega_{a,in})$, as a function of the inlet weight fraction, $\omega_{a,in}$. Thick black lines show profiles generated with transference coefficient increments of 5, while thin grey lines show intermediate cases. A red shaded area indicates when the salt molality exceeds the solubility, and a thick red line shows the maximum change in weight fraction for $\omega_{a,in} = 0.6$.

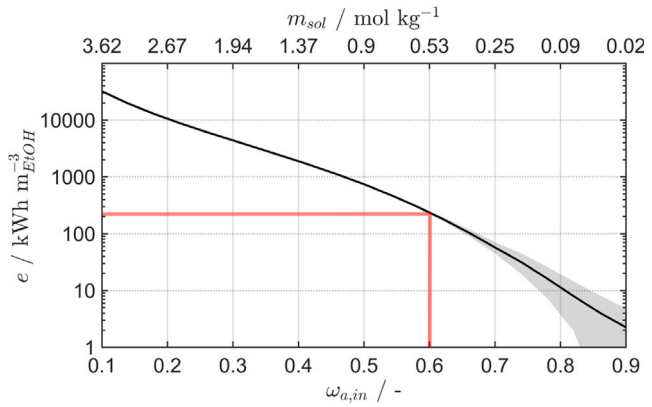

Fig. 7. The energy requirement of the demineralisation process, e, as a function of the inlet EtOH solvent weight fraction, $\omega_{a,in}$. The salt molality of the saturated feed is shown as the upper horizontal axis for all EtOH weight fractions. The solid black line shows the mean energy requirement with t_w in the range 0–20, whereas the grey shaded area shows the variance due to the water transference coefficient. A thick red line shows the energy requirement for $\omega_{a,in} = 0.6$.

The case of an individual membrane water transference coefficient of 11 is improbable for Selemion CMVN cation- and AMVN anion-exchange membranes in KCl electrolyte mixtures. A total of 22 moles of water are then transported from the feed to the draw channel of each unit cell per mole of electrons in the outer circuit. Water transference coefficients of around 4 have been found for these membranes in solutions of KCl and H_2O [39]. It is likely possible to engineer a membrane with a higher water transference coefficient for the target salt while keeping the EtOH transference coefficient low, considering the variance in water transference coefficients shown in Table 1.

The obtainable EtOH solvent weight fraction difference for the electrodialysis process is shown in Fig. 6 for various inlet weight fractions. Each line represents a unique combination of solvent transference coefficients. With an inlet EtOH weight fraction of $\omega_a = 0.6$, membrane transference coefficients of $t_w = 11$ and $t_a = 0$ lead to a weight fraction

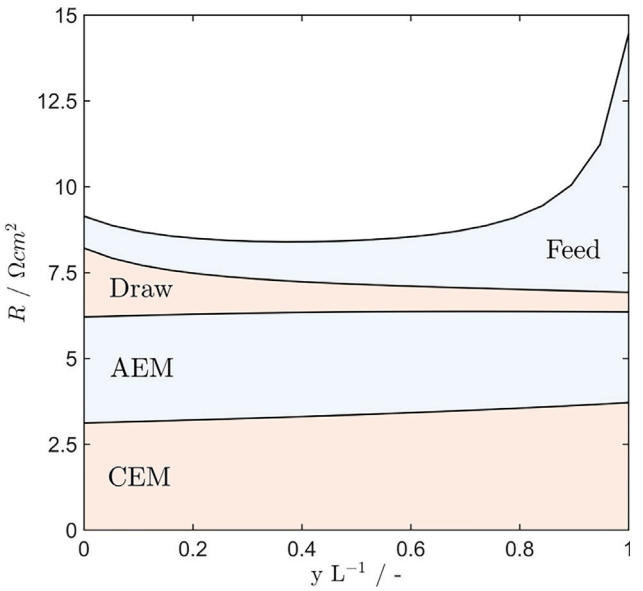

Fig. 8. The cumulative area resistance, R, of a unit cell at all positions from inlet to outlet, showing contributions from the anion-exchange membrane (AEM), cation exchange membrane (CEM), draw and feed channels. Generated for $\omega_{a,in} = 0.6$, $t_w = 11$ and $t_a = 0$.

difference of roughly 0.18 when the feed is almost completely demineralised, as shown by the red line. In general, the higher the initial EtOH weight fraction, the higher the membrane water transference coefficient must be in order to obtain an appreciable weight fraction difference.

The energy requirement, for one unit cell and the electrode system, to demineralise the feed channel mixture is shown in Fig. 7. It is shown in terms of energy per volume EtOH exiting the feed channel, so that adding additional unit cells will decrease the energy requirement slightly by reducing the relative contribution from the electrode system. It is indeed possible to add additional unit cells to the electrodialysis stack in order to up-scale the production capacity. Generally, the energy requirement to demineralise the feed mixture is high, above 1000 kWh m^{-3}_{EtOH}, when the initial salt content is above 1 mol kg^{-1}. A more probable starting weight fraction of EtOH is around 0.6–0.7 for the saturated mixtures that have been subject to hydrometallurgical salt recycling. For these mixtures, increasing the EtOH weight fraction by 0.1–0.2 may therefore be possible at an energy requirement of 60–200 kWh m^{-3}_{EtOH}. Comparatively, the energy consumption for production of anhydrous ethanol by distilling feed mixtures of ω_a = 0.05–0.1 EtOH falls in the range 1000–4200 kWh m^{-3}_{EtOH} [19]. Distillation allows for the separation of EtOH at a high purity from low starting weight fractions, such that these numbers are not directly comparable. The evaporation enthalpy of pure EtOH, however, is around 190 kWh m^{-3}_{EtOH} [20]. The electrodialysis concept is therefore unsuitable for low starting fractions of EtOH, requiring a higher energy input and producing significantly less pure EtOH than conventional distilliation. For high EtOH solvent weight fractions in the feed, such as residual mixtures from antisolvent precipitation, the concept is more interesting. Demineralising a saturated mixture at the EtOH solvent weight fraction of $\omega_a = 0.7$ can increase the weight fraction to $\omega_a = 0.81$ requiring 73 kWh m^{-3}_{EtOH} if the membrane transference coefficients are $t_w = 15$ and $t_a = 0$. The suitability of the process depends heavily on the salt concentration and the EtOH purity requirements.

The energy requirement is for most cases dominated by the ohmic contribution, as opposed to the contribution from the reversible electric potential given by the last two terms of Eq. (7). Only at $\omega_{a,in} = 0.8$ and above does the reversible electric potential contribution attain and

exceed the ohmic contribution. The area resistance of each subsystem of a unit cell is shown in Fig. 8 for the highlighted case in Fig. 7. For this example, 258 kWh m^{-3}_{EtOH} is required for the demineralisation of the feed. The ohmic resistance of the unit cell is dominated by the contributions from the membranes, in large part due to the membrane thickness. Only by the outlet of the cell, when the salt concentration in the feed is close to depleted, does the resistance contribution of the feed channel increase drastically. Reducing the membrane thickness for both the AEM and the CEM, from 100 μm to 50 μm, reduces the energy requirement to 170 kWh m^{-3}_{EtOH}. Reducing the channel thickness, from 270 μm to 135 μm, leads to an energy requirement of 220 kWh m^{-3}_{EtOH}. Both reductions are due to a reduced ohmic contribution for shorter electric current pathways. There is much to gain in terms of energy requirement by optimising the spatial dimensions of the cell.

For the application of the process to a mixture of for example Li_2SO_4, H_2SO_4, H_2O and EtOH from the hydrometallurgical recycling of Li-ion batteries, parameters of primary importance are the component activity coefficients, salt solubility, as well as the transport properties of the membrane and bulk electrolyte mixtures. All parameters depend on the local temperature, pressure and composition [50]. The activity coefficients enter into the component chemical potentials, and therefore affect the cell reversible electric potential (last two terms of Eq. (7)) as well as the driving force for diffusion (Eq. (9)). Diffusive transport is relatively small compared to the transference due to electric current (10–1000 times smaller) and has been neglected in the present treatment. It is here mainly the energy requirement for the process that is affected by the chemical potentials, as seen by the grey shaded area in Fig. 7. For instance, at $\omega_{a,in} = 0.7$ the current density is relatively low due to the small amount of salt in the saturated mixture. With $t_w = 5$ for each membrane in the unit cell, the contribution from the reversible electric potential is around 0.3% of the electrodialysis power density. It increases to roughly 28% if $t_w = 15$ due to the work required to transport extra water from the feed to the draw. However, this contribution can be lowered by increasing the amount of salt in the draw mixture in order to reduce the water activity. Therefore, at high EtOH solvent weight fractions the chemical potentials and activity coefficients of components are relatively important for the overall energy requirement, but they appear unlikely to affect the process to the same degree as the system transport properties, regardless of composition.

Applied to a feed mixture of Li_2SO_4, H_2SO_4, H_2O and EtOH means that divalent ions like SO_4^{2-} are present. For Nafion membranes, divalent ions such as Mg^{2+} have been shown to exhibit water transference coefficients of around 14 [40,62]. Moreover, the transference coefficients are defined per Coulomb of charge, such that a membrane water transference coefficient of 14 for a divalent ion means the ion carries 28 water molecules across the membrane. This may aid the efficacy of the membrane water transport. Furthermore, since the variance in water transference numbers depends on both composition and membrane characteristics, as shown in Table 1, it appears likely that ion-exchange membranes can be tailored for high water transference with a high rejection of EtOH or other antisolvents.

Aqueous mixtures of Li_2SO_4 have shown similar electric conductivities to mixtures of KCl up to 1 mol kg^{-1}, but up to 4 times lower at 3 mol kg^{-1} [63]. This will increase the process energy requirement relative to KCl. However, the conductivity also increases with temperature, providing an opportunity for the reduction of the required energy to demineralise the feed by operating the process above room temperature.

The aqueous mixture leftover from hydrometallurgical salt recovery will be acidic from the leaching process. The acid, e.g. H_2SO_4, also needs to be separated from the EtOH, and ions from the dissociated acid will also carry water molecules across the ion-exchange membranes. The dependence of the salt solubility on the concentration of acid is then also of importance. Gómez-García et al. measured the KCl solubility in mixtures of KCl−HCl−H_2O-EtOH, and found that addition

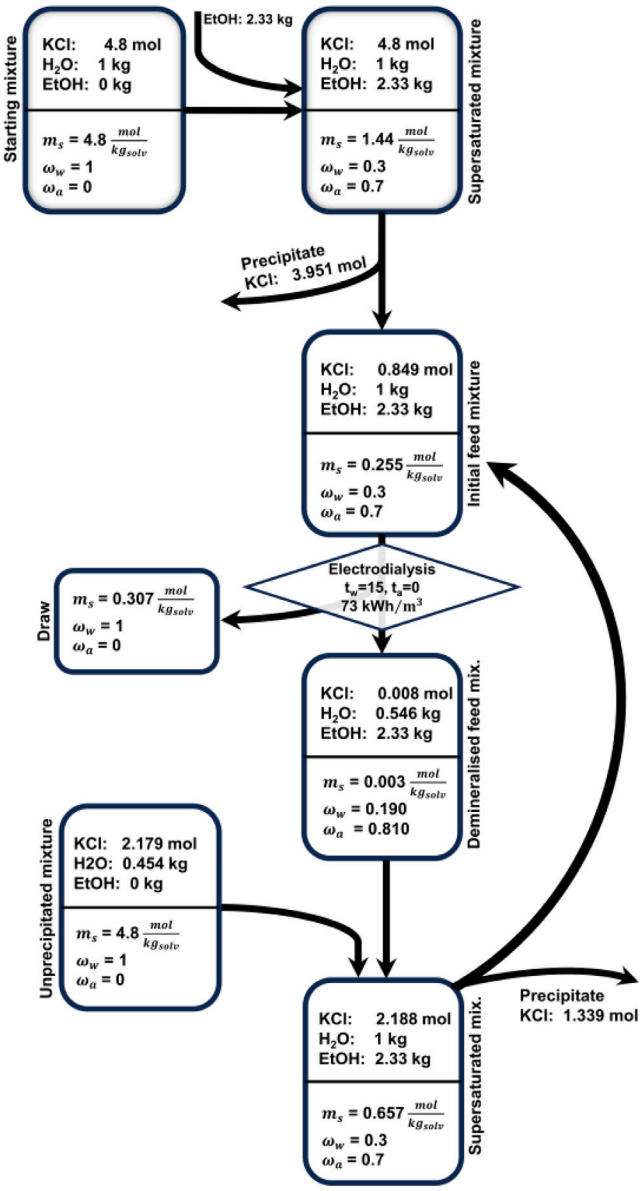

Fig. 9. Flowchart detailing the compositions of an example cyclic process involving antisolvent recycling by electrodialysis.

of HCl reduced the solubility of KCl. EtOH has also been shown to reduce the solubility of aqueous Li_2SO_4 [64], which is necessary for the antisolvent precipitation step in the recycling process. In summary, the interactions between the various parameters are complex and the fundamental parameters of relevance must be measured. The model results and current literature suggests that applying the process to a mixture e.g. Li_2SO_4, H_2SO_4, H_2O and EtOH can yield a purification of the antisolvent, mainly dependent on appropriate membrane transference coefficients. Future studies on this demineralisation concept should tackle the complex quaternary mixture consisting of a salt, water, antisolvent and acid.

4.2. Process considerations

Deploying electrodialysis for antisolvent recovery to the point where one has pure antisolvent appears infeasible in the investigated cases, primarily due to scaling issues and the need for $t_w > 20$. Moreover, it is unlikely that complete demineralisation of the antisolvent feed

happens in reality in the electrodialysis process, due to substantial concentration polarisation in the feed channel and increased ohmic energy contributions. Therefore a loop of the processed antisolvent fed back to the precipitation reactor will contain some residual water and some residual metal salts. Any incomplete separation of components is negative for the process, but a cyclic process may still be viable with only partial separation.

An example process, based on the EtOH weight fraction of $\omega_a = 0.7$ used by Aktas et al., is shown in Fig. 9. As long as the unprecipitated mixture is sufficiently concentrated in salt, the addition of the demineralised feed mixture will lead to the desired precipitation. The resulting precipitated mixture may then be used as the feed mixture for the next electrodialysis process. Per mole of KCl precipitated in the example loop, the electrodialysis unit consumes 0.161 kWh $\text{mol}_{\text{KCl}}^{-1}$. The draw effluent from the electrodialysis cell has its salt concentration increased from 0.1 to 0.307 mol kg^{-1}. Ideally, this draw mixture is reused until the salt concentration is suitable for precipitation by addition of the demineralised feed mixture.

For an eventual realisation of the proposed process, it is also necessary to thoroughly investigate the ion-exchange membrane ageing and degradation. Polymer plasticisation may be a problem when in contact with EtOH-containing electrolyte mixtures [65]. The issue of membrane lifetime goes hand-in-hand with the cost of the process [66], which is suggested as one of the next steps in the evaluation of the electrodialysis concept.

5. Conclusions

Antisolvent precipitation is a hydrometallurgical process that may serve as a potent recycling strategy for Li-ion batteries, especially so when aided with electrodialysis for efficient reuse of the antisolvent. In this paper, a theoretical framework and simulation of an electrodialysis unit cell for the demineralisation of an EtOH, water and KCl mixture have been investigated. These components were chosen due to availability of thermodynamic data. The co-migration of water and EtOH, quantified by the transference coefficients, and the initial solvent weight fraction of EtOH (which also defines the molar flow rate of salt in the saturated solution) served as the main variables of interest.

The study suggests that electrodialysis may be a competitive process for the partial purification of EtOH in the intermediate weight fraction range. The saturated mixture produced by the antisolvent precipitation process, with $\omega_{a,in} = 0.7$, may be demineralised and the EtOH solvent weight fraction increased to $\omega_a \approx 0.81$ by the use of ion-exchange membranes with $t_w = 15$ and $t_a = 0$. Such a process required around 73 kWh $\text{m}_{\text{EtOH}}^{-3}$, but the water transference coefficient cannot be higher before scaling occurs. An example process scheme was developed, showing that a cyclic process involving electrodialysis appears possible, producing solid salt at an energy requirement of around 0.161 kWh $\text{mol}_{\text{KCl}}^{-1}$.

This study explores an application of electrodialysis in which the co-transport of water through ion-exchange membranes and rejection of EtOH are desirable. Measurements of the coupling between solvents and charge transport in ion-exchange membranes are needed to further develop this concept. Additionally, such data needs to be measured for the relevant mixture compositions, e.g. Li^+ and acid-containing solutions, in order to design suitable membranes for the lithium-ion battery recycling process. The thermodynamic properties of those components must also be measured to evaluate the electrodialysis concept for that case. Desired membranes for this process must efficiently reject the antisolvent, while letting significant amounts of water pass alongside ions in a low resistance manner as part of the charge conduction process.

CRediT authorship contribution statement

Simon B.B. Solberg: Writing – original draft, Visualization, Validation, Software, Project administration, Methodology, Investigation, Formal analysis, Data curation, Conceptualization. **Lucía Gómez-Coma:** Writing – original draft, Investigation, Data curation. **Øivind Wilhelmsen:** Writing – review & editing, Supervision, Project administration, Funding acquisition. **Kerstin Forsberg:** Writing – original draft, Supervision, Project administration. **Odne S. Burheim:** Writing – original draft, Supervision, Resources, Project administration, Funding acquisition, Conceptualization.

Declaration of competing interest

The authors declare the following financial interests/personal relationships which may be considered as potential competing interests: Øivind Wilhelmsen reports financial support was provided by Research Council of Norway. If there are other authors, they declare that they have no known competing financial interests or personal relationships that could have appeared to influence the work reported in this paper.

Data availability

Data will be made available on request.

Acknowledgements

The authors are grateful for support and funding from the ENERSENSE research initiative (Grant Number (68024013) at the Norwegian University of Science and Technology, and the Department of Energy and Process Engineering through the project number 81772020. Ø.W. acknowledges funding from the Research Council of Norway (RCN), the Center of Excellence Funding Scheme, Project No. 262644, PoreLab. The authors also wish to thank Eirun H. Birkeland for conducting measurements of diffusion coefficients, and Joachim W. Grieg for conducting measurements of membrane and electrolyte solution conductivity.

Appendix A. Diffusion coefficient measurements

Aqueous mixtures of KCl (for analysis EMSURE, supplied by Merck) and EtOH (≥96% (V/V) TechniSolv, supplied by VWR Chemicals) were prepared using de-ionised water with a conductivity of 5.5 μS m^{-1}. Cation- and anion-exchange membranes of types CMVN and AMVN were supplied by AGC Engineering Co. Ltd. in Na^+ and Cl^- forms, respectively. By storing in mixtures of 0.1 mol kg^{-1} KCl for a minimum of one week, the CEMs were converted to K^+ form. Solutions were refreshed once every week for four weeks.

The diffusion coefficient of EtOH in Selemion CMVN and AMVN membranes were estimated by measuring the EtOH and water concentrations and diffusion fluxes through an ion-exchange membrane separating two mixtures of different EtOH fractions with no added salt. The ion-exchange membrane had an area of 15.9 cm^2 exposed to the solutions, and both compartment volumes were 150 mL which did not vary appreciably during the measurement. As no salt was added, the coupling between salt and EtOH/water fluxes was not measured in this estimate of the diffusion coefficients. The measurement cell is described by:

$$H_2O \quad \| \quad H_2O(\omega_w), \quad EtOH(\omega_a)$$

where $\|$ denotes the membrane, ω_a and ω_w are the weight fractions of EtOH and H_2O respectively, which are related through: $\omega_w + \omega_a = 1$. The weight fraction of EtOH was estimated by measuring the refractive index (RI) of the mixture. In the range of $\omega_a = 0 - 0.3$ and the absence

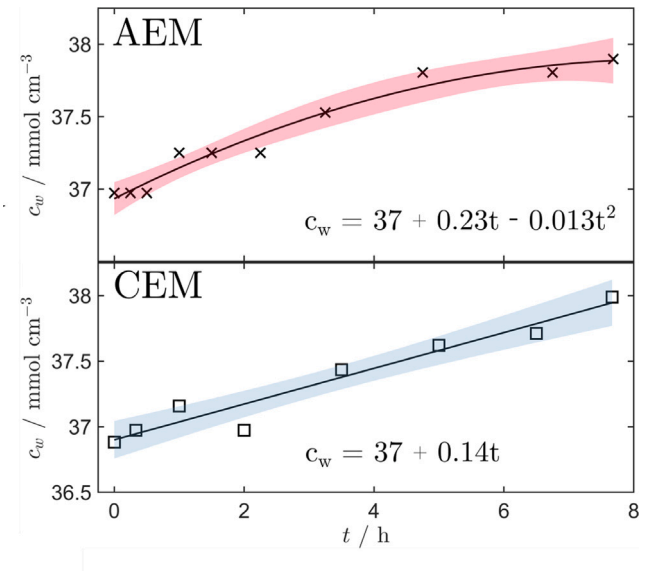

Fig. A.10. Concentration of water, c_w, on the mixed solvent side as function of time, t, when separated from a pure water compartment by a Selemion AMVN (AEM) or a Selemion CMVN (CEM). The initial EtOH weight fraction was $\omega_a = 0.3$. Regressions are presented with 95% confidence intervals as red and blue shaded areas for the AEM and CEM respectively.

of salt, a linear relation is produced to relate the RI to the EtOH weight fraction, which is well described by the empirical relation:

$$100\omega_a = 1560.5 \times \mathrm{RI} - 2078.6 \tag{A.1}$$

Furthermore, the density of EtOH-H_2O-KCl mixtures has been measured by Galleguillos et al. [67], which yielded a data set that is well described by:

$$\begin{aligned}\rho =& 0.9927 - 0.2588x_a - 0.2794x_a^2 + 0.5619x_a^3 \\ &+ 2.407x_s - 4.836x_a x_s + 5.072x_a^2 x_s\end{aligned} \tag{A.2}$$

where x_a and x_s are the mole fractions of EtOH and KCl respectively. The concentration of water, c_w, is related to the mole fraction through: $c_w = \rho x_w / \bar{M} = \rho\omega_w / M_w$, where $\bar{M}$ is the average molar mass of the mixture. The derivative of the concentration with respect to time yields the flux, and the Fick diffusion coefficients, D_{kw}, of component k is calculated using Eq. (10) in the absence of salt:

$$D_{kw} = -\delta_m \left(\frac{J_k}{\Delta c_w}\right)_{j=\Delta c_s=0} = \frac{\frac{\partial c_k}{\partial t}\frac{V}{A_m}\delta_m}{\Delta c_w} \tag{A.3}$$

where the concentration and flux of component k are c_k and J_k, V is the volume of the compartment receiving the component flux, δ_m is the membrane thickness, Δc_w is the water concentration difference across the membrane, and A_m is the membrane area.

The estimated water concentration in the mixed solvent compartment is given as a function of time in Fig. A.10 for the AEM and CEM respectively. The RI of the compartment containing pure water did not change over the course of the eight hour duration of the experiment. We interpret this as indicating that diffusion of EtOH is negligible for both membranes, i.e. $D_{aw} \approx 0$. An estimate of the water diffusion coefficient in the relevant membranes is taken as the average of the calculated values, which are found as: $D_{ww}^{\mathrm{AEM}} = 1.8 \times 10^{-7} \pm 0.7 \times 10^{-7}$ and $D_{ww}^{\mathrm{CEM}} = 2.0 \times 10^{-7} \pm 0.4 \times 10^{-7}$ cm^2 s^{-1}, where the uncertainty is reported as the double standard deviation.

Appendix B. Electric conductivity measurements

The electric conductivity of the aqueous mixture was measured using a Portavo 907 multi-meter in combination with a Knick SE680 toroidal conductivity sensor. Aqueous mixtures of KCl, H_2O and EtOH were prepared with the same chemicals and procedure as the diffusion coefficient measurements presented in Appendix A. Measured values are reported in Table B.3, and they are well represented by a polynomial on the form:

Table B.3
Measured electric conductivity, κ, of the ternary EtOH/H_2O/KCl mixture.

ω_a	m_s mol kg^{-1}	κ_{mix} mS cm^{-1}
0	0.1	12.6
0	0.5	54.1
0	1	102.6
0	1.5	145.6
0	4.5	347.7
0.1	0.5	38.8
0.2	0.5	29.1
0.3	0.5	22.2
0.1	1	73.7
0.2	1	53.7
0.3	1	41.2
0.1	1.5	106.9
0.2	1.5	78.8
0.3	1.5	65.8

$$\begin{aligned}\kappa_{\mathrm{mix}} =& 108.7m_s - 6.997m_s^2 - 348.1m_s\omega_a \\ &+ 23.96m_s^2\omega_a + 428.4m_s\omega_a^2\end{aligned} \tag{B.1}$$

where the electric conductivity has a positive dependence on salt concentration, but a negative dependence on the fraction of EtOH.

The electric conductivity of the Selemion CMVN and AMVN ion-exchange membranes were measured after soaking in various mixture compositions for a minimum of seven days in order to reach equilibrium between the external and internal electrolyte solutions. Membrane conductivities were determined by measuring the electrochemical impedance of stacks of wetted membranes. A Gamry Interface 5000E potentiostat was used for impedance measurements. Ion-exchange membranes in stacks of three to five pieces were confined between two Pt-electrodes, between which an alternating current was imposed. The ohmic resistance of the system is obtained when the imaginary part of the impedance is zero, and the contribution of the membrane is isolated by creating a linear regression of resistance as function of membrane stack thickness. The experimental process was described in detail by Krakhella et al. [68]. Measured values are reported in Table B.4

Both the Selemion CMVN and AMVN (cation- and anion-exchange membranes respectively) do not have a statistically significant dependence on the external concentration of salt in these measurements. The cation-exchange membrane electric conductivity is described to a sufficient accuracy by the following expression:

$$\kappa_{\mathrm{CEM}} = 4.752 - 5.16\omega_a \tag{B.2}$$

and the anion-exchange membrane is described to a sufficient accuracy by the following expression:

$$\kappa_{\mathrm{AEM}} = 8.867 - 36.8\omega_a + 60.58\omega_a^2 \tag{B.3}$$

where both types of membranes exhibit a reduction of electric conductivity with increasing fraction of EtOH.

Appendix C. Solubility in the ternary mixture

The solubility of KCl in aqueous mixtures with and without EtOH is well documented in the literature [69–73]. Measurement data from standard temperature and pressure experiments are shown in Fig. C.11. The literature data is well represented by a regression that is linear in the regression coefficients:

$$\begin{aligned}\log_{10}(m_{sol}) =& 1.66 + 1.02\omega_a - 1.03\omega_a^2 + 1.84\omega_a^3 - 3.73\omega_a^4 \\ &- \frac{293}{T} - 647\frac{\omega_a}{T} + 259\frac{\omega_a^3}{T}\end{aligned} \tag{C.1}$$

Table B.4
Measured electric conductivity, κ, of the Selemion CMVN (CEM) and AMVN (AEM) in equilibrium with an external EtOH/H_2O/KCl mixture.

ω_a	m_s mol kg^{-1}	κ_{CEM} mS cm^{-1}	κ_{AEM} mS cm^{-1}
0	0.5	9.13	5.10
0.1	0.5	4.37	4.13
0.2	0.5	5.26	4.04
0.3	0.5	3.12	3.70
0	1	8.32	4.92
0.1	1	5.90	3.79
0.2	1	3.92	3.48
0.3	1	3.00	2.70
0	1.5	9.45	4.50
0.1	1.5	5.73	4.43
0.2	1.5	3.75	3.57
0.3	1.5	3.18	3.38

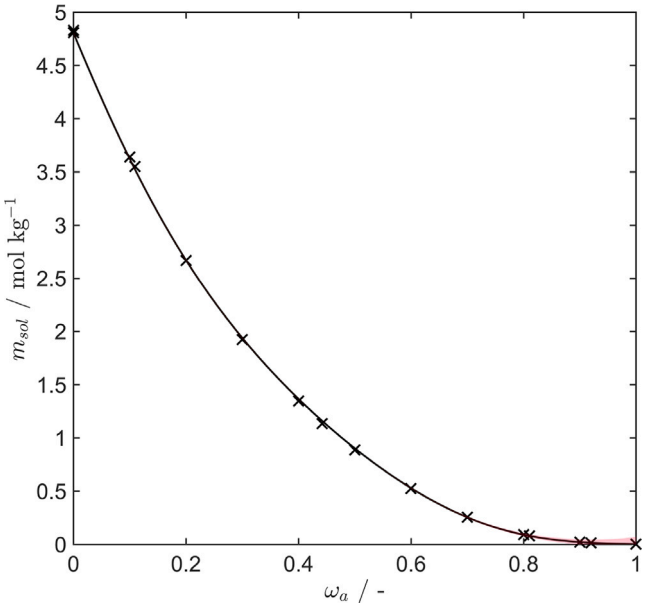

Fig. C.11. Solubility of KCl, m_{sol}, in aqueous mixtures with EtOH solvent weight fractions, w_a. A 95% confidence interval for the regression is illustrated by the red shaded area.

where m_{sol} is the KCl solubility in mol kg^{-1}, ω_a is the solvent weight fraction of EtOH subject to $\omega_a + \omega_w = 1$, and T is the absolute temperature of the mixture.

References

[1] M.M. Rana, M. Uddin, M.R. Sarkar, S.T. Meraj, G.M. Shafiullah, S.M. Muyeen, M.A. Islam, T. Jamal, Applications of energy storage systems in power grids with and without renewable energy integration - A comprehensive review, J. Energy Storage 68 (2023) http://dx.doi.org/10.1016/j.est.2023.107811.

[2] M.Y. Suberu, M.W. Mustafa, N. Bashir, Energy storage systems for renewable energy power sector integration and mitigation of intermittency, Renew. Sustain. Energy Rev. 35 (2014) 499–514, http://dx.doi.org/10.1016/j.rser.2014.04.009.

[3] R. Haas, C. Kemfert, H. Auer, A. Ajanovic, M. Sayer, A. Hiesl, On the economics of storage for electricity: Current state and future market design prospects, Wiley Interdiscip. Rev.: Energy Environ. 11 (2022) http://dx.doi.org/10.1002/wene.431.

[4] E. Borri, A. Tafone, G. Zsembinszki, G. Comodi, A. Romagnoli, L.F. Cabeza, Recent trends on liquid air energy storage: A bibliometric analysis, Appl. Sci. (Switz.) 10 (2020) http://dx.doi.org/10.3390/APP10082773.

[5] M.R. Chakraborty, S. Dawn 2, P.K. Saha, J.B. Basu, T.S. Ustun, A comparative review on energy storage systems and their application in deregulated systems, Batteries 8 (2022) http://dx.doi.org/10.3390/batteries8090124.

[6] R. Li, R. Deng, Z. Wang, Y. Wang, G. Huang, J. Wang, F. Pan, The challenges and perspectives of developing solid-state electrolytes for rechargeable multivalent battery, J. Solid State Electrochem. (2023) http://dx.doi.org/10.1007/s10008-023-05426-9.

[7] Z. Lv, P. Wang, J. Wang, S. Tian, T. Yi, Key challenges, recent advances and future perspectives of rechargeable lithium-sulfur batteries, J. Ind. Eng. Chem. 124 (2023) 68–88, http://dx.doi.org/10.1016/j.jiec.2023.04.025.

[8] M. Zhang, L. Wang, H. Xu, Y. Song, X. He, Polyimides as promising materials for lithium-ion batteries: A review, Nano-Micro Lett. 15 (2023) http://dx.doi.org/10.1007/s40820-023-01104-7.

[9] C. Xu, Q. Dai, L. Gaines, M. Hu, A. Tukker, B. Steubing, Future material demand for automotive lithium-based batteries, Commun. Mater. 1 (2020) 99, http://dx.doi.org/10.1038/s43246-020-00095-x.

[10] T. Fujita, H. Chen, K. Wang, C. He, Y. Wang, G. Dodbiba, Y. Wei, Reduction, reuse and recycle of spent Li-ion batteries for automobiles: A review, Int. J. Miner. Metall. Mater. 28 (2021) 179–192, http://dx.doi.org/10.1007/s12613-020-2127-8.

[11] Y. Ding, Z.P. Cano, A. Yu, J. Lu, Z. Chen, Automotive li-ion batteries: Current status and future perspectives, Electrochem. Energy Rev. 2 (2019) 1–28, http://dx.doi.org/10.1007/s41918-018-0022-z.

[12] J. Neumann, M. Petranikova, M. Meeus, J.D. Gamarra, R. Younesi, M. Winter, S. Nowak, Recycling of lithium-ion batteries-current state of the art, circular economy, and next generation recycling, Adv. Energy Mater. 12 (2022) http://dx.doi.org/10.1002/aenm.202102917.

[13] H. Ali, H.A. Khan, M. Pecht, Preprocessing of spent lithium-ion batteries for recycling: Need, methods, and trends, Renew. Sustain. Energy Rev. 168 (2022) http://dx.doi.org/10.1016/j.rser.2022.112809.

[14] K. Du, E.H. Ang, X. Wu, Y. Liu, Progresses in sustainable recycling technology of spent lithium-ion batteries, Energy Environ. Mater. 5 (2022) 1012–1036, http://dx.doi.org/10.1002/eem2.12271.

[15] J. Mao, C. Ye, S. Zhang, F. Xie, R. Zeng, K. Davey, Z. Guo, S. Qiao, Toward practical lithium-ion battery recycling: adding value, tackling circularity and recycling-oriented design, Energy Environ. Sci. 15 (2022) 2732–2752, http://dx.doi.org/10.1039/d2ee00162d.

[16] W. Xuan, A. Chagnes, X. Xiao, R.T. Olsson, K. Forsberg, Antisolvent precipitation for metal recovery from citric acid solution in recycling of NMC cathode materials, Metals 12 (2022) http://dx.doi.org/10.3390/met12040607.

[17] C.Y. Wu, W. Wang, Application of antisolvent precipitation method for formulating excipient-free nanoparticles of psychotropic drugs, Pharmaceutics 14 (2022) http://dx.doi.org/10.3390/pharmaceutics14040819.

[18] S. Aktas, D. Fray, O. Burheim, J. Fenstad, E. Açma, Recovery of metallic values from spent Li ion secondary batteries, Miner. Process. Extr. Metall. 115 (2) (2006) 95–100.

[19] S. Kumar, N. Singh, R. Prasad, Anhydrous ethanol: A renewable source of energy, Renew. Sustain. Energy Rev. 14 (2010) 1830–1844, http://dx.doi.org/10.1016/j.rser.2010.03.015.

[20] S.M. Richard M. Stephenson, Handbook of the Thermodynamics of Organic Compounds, Springer Dordrecht, ISBN: 978-94-009-3173-2, 2012, http://dx.doi.org/10.1007/978-94-009-3173-2.

[21] J.J. Feria-Díaz, F. Correa-Mahecha, M.C. López-Méndez, J.P. Rodríguez-Miranda, J. Barrera-Rojas, Recent desalination technologies by hybridization and integration with reverse osmosis: A review, Water 13 (10) (2021) http://dx.doi.org/10.3390/w13101369.

[22] Ö. Tekinalp, P. Zimmermann, O.S. Burheim, L. Deng, Designing monovalent selective anion exchange membranes for the simultaneous separation of chloride and fluoride from sulfate in an equimolar ternary mixture, J. Membr. Sci. 666 (2023) 121148, http://dx.doi.org/10.1016/j.memsci.2022.121148.

[23] P. Zimmermann, Ö. Tekinalp, S.B.B. Solberg, Ø. Wilhelmsen, L. Deng, O.S. Burheim, Limiting current density as a selectivity factor in electrodialysis of multi-ionic mixtures, Desalination 558 (2023) 116613, http://dx.doi.org/10.1016/j.desal.2023.116613.

[24] A.Y. Bagastyo, A.Z. Sinatria, A.D. Anggrainy, K.A. Affandi, S.W.T. Kartika, E. Nurhayati, Resource recovery and utilization of bittern wastewater from salt production: a review of recovery technologies and their potential applications, Environ. Technol. Rev. 10 (2021) 294–321, http://dx.doi.org/10.1080/21622515.2021.1995786.

[25] A. Campione, L. Gurreri, M. Ciofalo, G. Micale, A. Tamburini, A. Cipollina, Electrodialysis for water desalination: A critical assessment of recent developments on process fundamentals, models and applications, Desalination 434 (2018) 121–160, http://dx.doi.org/10.1016/j.desal.2017.12.044, Reviews on Research and Development in Desalination.

[26] F. Borges, H. Roux-de Balmann, R. Guardani, Investigation of the mass transfer processes during the desalination of water containing phenol and sodium chloride by electrodialysis, J. Membr. Sci. 325 (1) (2008) 130–138, http://dx.doi.org/10.1016/j.memsci.2008.07.017.

[27] P. Zimmermann, K. Wahl, Ö. Tekinalp, S.B.B. Solberg, L. Deng, Ø. Wilhelmsen, O.S. Burheim, Selective recovery of silver ions from copper-contaminated effluents using electrodialysis, Desalination 572 (2024) 117108, http://dx.doi.org/10.1016/j.desal.2023.117108.

[28] L. Bazinet, Electrodialytic phenomena and their applications in the dairy industry: A review, Crit. Rev. Food Sci. Nutr. 45 (4) (2005) 307–326, http://dx.doi.org/10.1080/10408690490489279.

[29] E. Singlande, H. Roux-de Balmann, X. Lefevbre, M. Sperandio, Improvement of the treatment of salted liquid waste by integrated electrodialysis upstream biological treatment, Desalination 199 (1) (2006) 64–66, http://dx.doi.org/10.1016/j.desal.2006.03.020, Euromembrane 2006.

[30] S. Galier, H.R. Balmann, Demineralization of glucose solutions by electrodialysis: Influence of the ionic composition on the mass transfer and process performances, Can. J. Chem. Eng. 93 (2) (2015) 378–385, http://dx.doi.org/10.1002/cjce.22076.

[31] T. Elisseeva, V. Shaposhnik, I. Luschik, Demineralization and separation of amino acids by electrodialysis with ion-exchange membranes, Desalination 149 (1) (2002) 405–409, http://dx.doi.org/10.1016/S0011-9164(02)00763-4.

[32] J. Shen, J. Duan, Y. Liu, Y. Lixin, X. Xing, Demineralization of glutamine fermentation broth by electrodialysis, Desalination 172 (2) (2005) 129–135, http://dx.doi.org/10.1016/j.desal.2004.05.010.

[33] V.H. Thang, W. Koschuh, K.D. Kulbe, S. Novalin, Detailed investigation of an electrodialytic process during the separation of lactic acid from a complex mixture, J. Membr. Sci. 249 (1) (2005) 173–182, http://dx.doi.org/10.1016/j.memsci.2004.08.033.

[34] A. Luiz, D.D. McClure, K. Lim, G. Leslie, H.G. Coster, G.W. Barton, J.M. Kavanagh, Potential upgrading of bio-refinery streams by electrodialysis, Desalination 415 (2017) 20–28, http://dx.doi.org/10.1016/j.desal.2017.02.023.

[35] A. Elmidaoui, F. Lutin, L. Chay, M. Taky, M. Tahaikt, M.R. Hafidi, Removal of melassigenic ions for beet sugar syrups by electrodialysis using a new anion-exchange membrane, Desalination 148 (1) (2002) 143–148, http://dx.doi.org/10.1016/S0011-9164(02)00668-9.

[36] F.G. Neytzell-de Wilde, Demineralization of a molassess distillery waste water, Desalination 67 (1987) 481–493, http://dx.doi.org/10.1016/0011-9164(87)90264-5.

[37] Ö. Tekinalp, P. Zimmermann, S. Holdcroft, O.S. Burheim, L. Deng, Cation exchange membranes and process optimizations in electrodialysis for selective metal separation: A review, Membranes 13 (6) (2023) http://dx.doi.org/10.3390/membranes13060566.

[38] T. Okada, H. Satou, M. Okuno, M. Yuasa, Ion and water transport characteristics of perfluorosulfonated ionomer membranes with H^+ and alkali metal cations, J. Phys. Chem. B 106 (6) (2002) 1267–1273, http://dx.doi.org/10.1021/jp013195l.

[39] S. Solberg, P. Zimmermann, Ø. Wilhelmsen, R. Bock, O.S. Burheim, Analytical treatment of ion-exchange permselectivity and transport number measurements for high accuracy, J. Membr. Sci. 685 (2023) 121904, http://dx.doi.org/10.1016/j.memsci.2023.121904.

[40] G. Xie, T. Okada, Water transport behavior in nafion 117 membranes, J. Electrochem. Soc. 142 (9) (1995) 3057, http://dx.doi.org/10.1149/1.2048686.

[41] A. Zlotorowicz, R. Strand, O. Burheim, Ø. Wilhelmsen, S. Kjelstrup, The permselectivity and water transference number of ion exchange membranes in reverse electrodialysis, J. Membr. Sci. 523 (2017) http://dx.doi.org/10.1016/j.memsci.2016.10.003.

[42] T.F. Fuller, J. Newman, Experimental determination of the transport number of water in nafion 117 membrane, J. Electrochem. Soc. 139 (5) (1992) 1332, http://dx.doi.org/10.1149/1.2069407.

[43] G. Xie, T. Okada, Characteristics of water transport in relation to microscopic structure in Nafion membranes, J. Chem. Soc. Faraday Trans. 92 (4) (1996) 663–669.

[44] Y.-H. Chiao, Z. Mai, W.-S. Hung, H. Matsuyama, Osmotically assisted solvent reverse osmosis membrane for dewatering of aqueous ethanol solution, J. Membr. Sci. 672 (2023) 121434, http://dx.doi.org/10.1016/j.memsci.2023.121434.

[45] P. Kanchanalai, R.P. Lively, M.J. Realff, Y. Kawajiri, Cost and energy savings using an optimal design of reverse osmosis membrane pretreatment for dilute bioethanol purification, Ind. Eng. Chem. Res. 52 (32) (2013) 11132–11141, http://dx.doi.org/10.1021/ie302952p.

[46] C. Liu, G. Dong, T. Tsuru, H. Matsuyama, Organic solvent reverse osmosis membranes for organic liquid mixture separation: A review, J. Membr. Sci. 620 (2021) 118882, http://dx.doi.org/10.1016/j.memsci.2020.118882.

[47] W. Kurniawan, D. Takaiwa, E. Yamamoto, K. Yasuoka, Separation of water–ethanol solutions with carbon nanotubes and electric fields, Phys. Chem. Chem. Phys. 18 (2016) 33310–33319, http://dx.doi.org/10.1039/C6CP06731J.

[48] C.Z. Liang, M. Askari, L.T. Choong, T.-S. Chung, Ultra-strong polymeric hollow fiber membranes for saline dewatering and desalination, Nature Commun. 12 (2021) 2338, http://dx.doi.org/10.1038/s41467-021-22684-1.

[49] L. Gurreri, A. Tamburini, A. Cipollina, G. Micale, Electrodialysis applications in wastewater treatment for environmental protection and resources recovery: A systematic review on progress and perspectives, Membranes 10 (2021) http://dx.doi.org/10.3390/membranes10070146.

[50] S. Kjelstrup, D. Bedeaux, Non-Equilibrium Thermodynamics of Heterogeneous Systems, World Scientific, Singapore, 2008.

[51] S. de Groot, P. Mazur, Non-Equilibrium Thermodynamics, in: Dover Books on Physics, Dover Publications, ISBN: 9780486647418, 1984.

[52] R. Yang, J. Demirgian, J.F. Solsky, E.J. Kikta, J.A. Marinsky, Mean molal activity of sodium chloride, potassium chloride, and cesium chloride in ethanol-water mixtures, J. Phys. Chem. 83 (21) (1979) 2752–2761, http://dx.doi.org/10.1021/j100484a013.

[53] A.J. Dill, L.M. Itzkowitz, O. Popovych, Standard potentials of potassium electrodes and activity coefficients and medium effects of potassium chloride in ethanol-water solvents, J. Phys. Chem. 72 (13) (1968) 4580–4586, http://dx.doi.org/10.1021/j100859a036.

[54] P.R. Mussini, T. Mussini, A. Perelli, S. Rondinini, A. Vertova, Thermodynamics of the cell: MexHg(1-x)-MeCl(m)-AgCl-Ag (Me = Na,K,Cs) in (ethanol + water) solvent mixtures, J. Chem. Thermodyn. 27 (3) (1995) 245–251, http://dx.doi.org/10.1006/jcht.1995.0022.

[55] A. Lopes, F. Farelo, M.I.A. Ferra, Activity coefficients of potassium chloride in water–ethanol mixtures, J. Solut. Chem. 28 (1999) 117–131, http://dx.doi.org/10.1023/A:1021746012370.

[56] X. Liu, A. Martín-Calvo, E. McGarrity, S.K. Schnell, S. Calero, J.-M. Simon, D. Bedeaux, S. Kjelstrup, A. Bardow, T.J.H. Vlugt, Fick diffusion coefficients in ternary liquid systems from equilibrium molecular dynamics simulations, Ind. Eng. Chem. Res. 51 (30) (2012) 10247–10258, http://dx.doi.org/10.1021/ie301009v.

[57] P.A. Rock, The standard oxidation potential of the ferrocyanide-ferricyanide electrode at 25° and the entropy of ferrocyanide ion, J. Phys. Chem. 70 (2) (1966) 576–580, http://dx.doi.org/10.1021/j100874a042.

[58] O.S. Burheim, F. Seland, J.G. Pharoah, S. Kjelstrup, Improved electrode systems for reverse electro-dialysis and electro-dialysis, Desalination 285 (2012) 147–152.

[59] J. Veerman, R.M. de Jong, M. Saakes, S.J. Metz, G.J. Harmsen, Reverse electrodialysis: Comparison of six commercial membrane pairs on the thermodynamic efficiency and power density, J. Membr. Sci. 343 (2009) 7–15, http://dx.doi.org/10.1016/j.memsci.2009.05.047.

[60] P. Zimmermann, S.B.B. Solberg, Ö. Tekinalp, J.J. Lamb, Ø. Wilhelmsen, L. Deng, O.S. Burheim, Heat to hydrogen by RED - reviewing membranes and salts for the RED heat engine concept, Membranes 12 (1) (2022) http://dx.doi.org/10.3390/membranes12010048.

[61] S.B.B. Solberg, P. Zimmermann, Ø. Wilhelmsen, J.J. Lamb, R. Bock, O.S. Burheim, Heat to hydrogen by reverse electrodialysis - using a non-equilibrium thermodynamics model to evaluate hydrogen production concepts utilising waste heat, Energies 15 (16) (2022) http://dx.doi.org/10.3390/en15166011.

[62] G. Xie, T. Okada, Pumping effects in water movement accompanying cation transport across nafion 117 membranes, Electrochim. Acta 41 (9) (1996) 1569–1571, http://dx.doi.org/10.1016/0013-4686(95)00391-6.

[63] A. Carton, F. Sobron, S. Bolado, J.I. Gerboles, Density, viscosity, and electrical conductivity of aqueous solutions of lithium sulfate, J. Chem. Eng. Data 40 (4) (1995) 987–991, http://dx.doi.org/10.1021/je00020a057.

[64] A. Carton, F. Sobron, S. Bolado, J. Tabares, Composition and density of saturated solutions of lithium sulfate + water + ethanol, J. Chem. Eng. Data 39 (1) (1994) 61–62, http://dx.doi.org/10.1021/je00013a017.

[65] L. Han, Aging and degradation of ion-exchange membranes, in: Membrane Technology Enhancement for Environmental Protection and Sustainable Industrial Growth, Springer International Publishing, Cham, 2021, pp. 27–38, http://dx.doi.org/10.1007/978-3-030-41295-1_3.

[66] Y.D. Raka, H. Karoliussen, K.M. Lien, O.S. Burheim, Opportunities and challenges for thermally driven hydrogen production using reverse electrodialysis system, Int. J. Hydrogen Energy 45 (2) (2020) 1212–1225, http://dx.doi.org/10.1016/j.ijhydene.2019.05.126.

[67] H.R. Galleguillos, M.E. Taboada, T.A. Graber, S. Bolado, Compositions, densities, and refractive indices of potassium chloride + ethanol + water and sodium chloride + ethanol + water solutions at (298.15 and 313.15) K, J. Chem. Eng. Data 48 (2) (2003) 405–410, http://dx.doi.org/10.1021/je020173z.

[68] K.W. Krakhella, R. Bock, O.S. Burheim, F. Seland, K.E. Einarsrud, Heat to H2: Using waste heat for hydrogen production through reverse electrodialysis, Energies 12 (18) (2019) http://dx.doi.org/10.3390/en12183428.

[69] S.P. Pinho, E.A. Macedo, Solubility of NaCl, NaBr, and KCl in water, methanol, ethanol, and their mixed solvents, J. Chem. Eng. Data 50 (1) (2005) 29–32, http://dx.doi.org/10.1021/je049922y.

[70] O. Chiavone-Filho, P. Rasmussen, Solubilities of salts in mixed solvents, J. Chem. Eng. Data 38 (3) (1993) 367–369, http://dx.doi.org/10.1021/je00011a009.

[71] L. Zhang, Q. Gui, X. Lu, Y. Wang, J. Shi, B.C.Y. Lu, Measurement of solid-liquid equilibria by a flow-cloud-point method, J. Chem. Eng. Data 43 (1) (1998) 32–37, http://dx.doi.org/10.1021/je970176p.

[72] R. Shearman, A. Menzies, The solubilities of potassium chloride in deuterium water and in ordinary water from 0 to 180 C, J. Am. Chem. Soc. 59 (185) (1937).

[73] A.A. Sunier, J. Baumbach, The solubility of potassium chloride in ordinary and heavy water, J. Chem. Eng. Data 21 (3) (1976) 335–336, http://dx.doi.org/10.1021/je60070a011.